Inorganic Chemistry

Article

pubs.acs.org/IC

DOSY NMR, X-ray Structural and Ion-Mobility Mass Spectrometric Studies on Electron-Deficient and Electron-Rich M_6L_4 Coordination Cages

Pia Bonakdarzadeh,[†] Filip Topić,[†] Elina Kalenius,[†] Sandip Bhowmik,[†] Sota Sato,[‡] Michael Groessl,[§] Richard Knochenmuss,[§] and Kari Rissanen*,[†]

[†]University of Jyväskylä, Department of Chemistry, Nanoscience Center, P.O. Box 35, FI-40014, University of Jyväskylä, Finland

[‡]AIMR, Department of Chemistry, and JST ERATO, Tohoku University, Aoba-ku, Sendai 980-8578, Japan

[§]Tofwerk AG, Uttigenstr. 22, 3600 Thun, Switzerland

Supporting Information

ABSTRACT: A novel modular approach to electron-deficient and electron-rich M_6L_4 cages is presented. From the same starting compound, via a minor modulation of the synthesis route, two C_3-symmetric ligands **L1** and **L2** with different electronic properties are obtained in good yield. The trifluoro-triethynylbenzene-based ligand **L1** is more electron-deficient than the well-known 2,4,6-tri(4-pyridyl)-1,3,5-triazine, while the trimethoxy-triethynylbenzene-based ligand **L2** is more electron-rich than the corresponding benzene analogue. Complexation of the ligands with cis-protected square-planar $[(dppp)Pt(OTf)_2]$ or $[(dppp)Pd(OTf)_2]$ corner-complexes yields two electron-deficient (**1a** and **1b**) and two electron-rich (**2a** and **2b**) M_6L_4 cages. The single crystal X-ray diffraction study of **1a** and **2a** confirms the expected octahedral shape with a ca. 2000 Å^3 cavity and ca. 11 Å wide apertures. The crystallographically determined diameters of **1a** and **2a** are 3.7 and 3.6 nm, respectively. The hydrodynamic diameters obtained from the DOSY NMR in $CDCl_3$:CD_3OD (4:1), and diameters calculated from collision cross sections (CCS) acquired by ion-mobility mass spectrometry (IM-MS) were for all four cages similar. In solution, the cage structures have diameters between 3.3 to 3.6 nm, while in the gas phase the corresponding diameters varied between 3.4 to 3.6 nm. In addition to the structural information the relative stabilities of the Pt_6L_4 and Pd_6L_4 cages were studied in the gas phase by collision-induced dissociation (CID) experiments, and the photophysical properties of the ligands **L1** and **L2** and cages **1a**, **1b**, **2a**, and **2b** were studied by UV−vis and fluorescence spectroscopy.

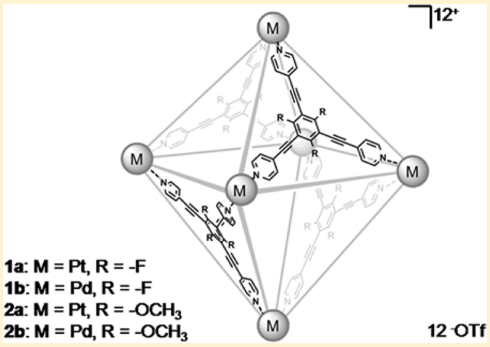

INTRODUCTION

Over the last 20 years, coordination-driven self-assembly has been demonstrated to be a highly efficient method to produce three-dimensional supramolecular architectures. Rational design of such discrete structures is based on structurally predesigned building blocks, viz. ligands and the known coordination geometries of specific metal cations. Consequently the coordination geometries of the metal ions (M^{n+}) and the number of the binding sites of ligands (L) and overall structure of the ligand define the geometry of the assembly.[1]

The simplest of "platonic solid" coordination cages are tetrahedron, cube, and octahedron.[1] Also "higher order" coordination polyhedra are known.[2] Tetrahedral coordination cages can be prepared by edge-directed self-assembly of C_2-symmetric bis-bidentate ligands or their subcomponents with suitable, usually octahedrally coordinated metal cations, leading to the M_4L_6 complex.[1c,d,3] An alternative route, face-directed self-assembly, uses C_3-symmetric tris-bidentate ligands which upon metal coordination lead to M_4L_4 tetrahedra.[1e,4] The cubic coordination cages can also be obtained by edge or face-directed self-assembly of bis-monodentate,[5] bis-bidentate,[6] tetrakis-monodentate,[7] or tetrakis-bidentate[8] ligands with suitable metal cations.

The pioneering work by Fujita[9] and Stang[10] has provided the basis for the M_6L_4 cages. Fujita's molecular paneling approach defines trigonal C_3-symmetric tris-monodentate *N*-donor ligands as "paneling ligands", which upon complexation with a proper metal cation, leads to M_6L_4, whereas Stang's approach uses "directional bonding", which under similar conditions leads to analogous M_6L_4 cages. The generally used metal cations are the cis-protected square-planar Pd(II) and Pt(II) "corner"-complexes with two labile anionic ligands (typically nitrates or triflates) at 90° angle available for *N*-ligand binding. The Fujita's approach uses mostly ethylenediamine as a protective group for the metal, whereas Stang's approach uses the more robust bisphosphino complex.[11] The directional bonding approach (Stang) defines the M_6L_4 cage as a truncated tetrahedron, where the ligands act as the faces of a tetrahedron, while the ditopic metals are placed in the middle of the edges,

Received: May 14, 2015
Published: June 3, 2015

DOI: 10.1021/acs.inorgchem.5b01082
Inorg. Chem. 2015, 54, 6055−6061

whereas the molecular paneling approach (Fujita) refers to M_6L_4 as an octahedron with the paneling ligands as the faces and the metal ions as the vertices.

Until now, eight trigonal C_3-symmetric tris-monodentate *N*-donor ligands with either pyridine or cyano groups as the donors have been used in the construction of M_6L_4 cages (Figure 1).[9,10,12] Additionally, there are other ligands, mostly

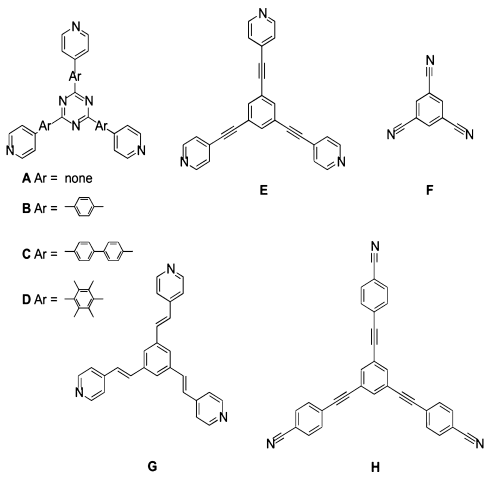

Figure 1. Similar ligands (**A**–**H**) previously used in M_6L_4 cages.[9,10,12]

nonplanar, used in M_6L_4 cages as well.[13] A common modification of the well-known electron-deficient triazine ligand (Figure 1, **A**)[9] toward larger-sized M_6L_4 cages has been the addition of aromatic ring(s) between the central triazine ring and the donor groups (Figure 1, **B**–**D**).[9,12a] A benzene core has been used together with ethynyl or ethenyl moieties (Figure 1, **E** and **G**).[10,12b,c] Cyano groups as *N*-donors have been used instead of pyridine in smaller (Figure 1, **F**)[12d] or larger (Figure 1, **H**)[12b] versions. Also, changing the protecting groups around the metal cation[10,12b,c,14] or the metal itself[12d,13c,15] has been another way of modifying the cages. Surprisingly the modification of the central benzene core (Figure 1, **E**)[10,12b,c] has not been explored. Herein we report the synthesis and characterization of two new C_3-symmetric ligands **L1** and **L2**, their self-assembly with Stang's Pt or Pd-corner-complexes,[11] [(dppp)Pt(OTf)$_2$] and [(dppp)Pd(OTf)$_2$] (dppp = 1,3-[bis(diphenylphosphino)]-propane), into M_6L_4 cages **1a**, **1b**, **2a**, and **2b** and their full characterization by NMR spectroscopy, single-crystal X-ray diffraction, mass spectrometry, ion-mobility mass spectrometry, UV–vis and fluorescence spectroscopy. To the best of our knowledge, this is the first time the size of coordination cages has been studied in three different states of matter as thoroughly, including also information by techniques such as DOSY NMR and IM-MS. The concerted use of three complementary structural techniques allows for the comparison of the sizes of the coordination cages in solution, solid state, and gas phase.

RESULTS AND DISCUSSION

Ligand Design and Self-Assembly of M_6L_4 Cages. Inspired by Stang et al.'s[10,12b,c] work on M_6L_4 coordination cages and the possibility to tune the properties of the central benzene ring, two C_3-symmetric target ligands, either electron-deficient with a trifluoro-triethynylbenzene core or electron-rich with a trimethoxy-triethynylbenzene core, were prepared starting from commercially available 1,3,5-trifluoro-2,4,6-triiodobenzene (Scheme 1) by adapting a known procedure.[16] The ligand **L1**, 1,3,5-tris[(4-pyridyl)ethynyl]-2,4,6-trifluoroben-

Scheme 1. Syntheses of Ligands and Self-Assembly of M_6L_4 Cages 1a, 1b, 2a, and 2b[a]

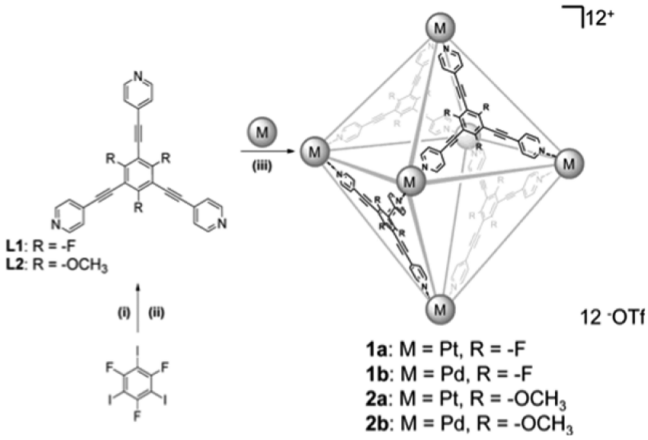

[a]Reaction conditions for ligand **L1**: (i) 4-ethynylpyridine, [Pd(PPh$_3$)$_2$Cl$_2$], CuI, *i*-Pr$_2$NH, 70 °C, 48 h, 41% and for ligand **L2**: (ii) (a) NaOCH$_3$, 1,3-dimethyl-2-imidazolidinone, r.t., 18 h, 69%, (b) same conditions as in (i) 59%. (iii) **L1** or **L2** (4 equiv), [(dppp)M(OTf)$_2$] (M = Pt, Pd; 6 equiv), CHCl$_3$:CH$_3$OH (4:1), 60 °C, 2 h.

zene, was prepared via Sonogashira coupling with 4-ethynylpyridine, while the ligand **L2**, 1,3,5-tris[(4-pyridyl)-ethynyl]-2,4,6-trimethoxybenzene, was synthesized by nucleophilic aromatic substitution followed by Sonogashira coupling (Scheme 1). The ethynyl spacers between the pyridine rings and the trifluoro- or trimethoxybenzene core make the ligands **L1** and **L2** and the resulting M_6L_4 cages larger than the corresponding M_6L_4 cages containing the ligand **A**, and at the same time allowing the ligand to adopt planar conformation needed for the successful cage formation. A small change in the synthesis protocol (Scheme 1) from the same starting material (1,3,5-trifluoro-2,4,6-triiodo-benzene) results in a modulation of the electron density of the benzene core. The trifluoro ligand **L1** is strongly electron-deficient, while the trimethoxy analogue **L2** is electron-rich. Using these ligands with cis-protected Stang's corner-complex[11] [(dppp)M(OTf)$_2$] (M = Pd or Pt) leads to four new large M_6L_4 octahedral cages **1a**, **1b**, **2a**, and **2b** (Scheme 1).

The electrostatic potential surfaces were calculated[17] for ligands **L1**, **L2**, triazine ligand **A**, and tris-ethynylbenzene ligand **E** (Figure 2). The strongly electron-withdrawing fluorine atoms at 2-, 4- and 6-positions, in addition to electron-withdrawing ethynyl moieties at 1-, 3-, and 5-positions, substantially decrease the electron density of the benzene core of ligand **L1** making it more electron-deficient than the triazine ligand **A** (Figure 2).

The trimethoxy ligand **L2**, on the other hand, has more electron-rich benzene core compared to the ligand **E** (Figure 2), due to the electron donating effect of methoxy groups (Figure 2). In addition to the molecular M_6L_4 cages, Fujita et al. have utilized the electron-deficiency of triazine ligand **A** in trapping electron-rich guests inside 3D coordination networks[18] and pillared coordination cages.[19]

The complexation of Pt- or Pd-corner complex (6 equiv) with ligand **L1** or **L2** (4 equiv) in CHCl$_3$:CH$_3$OH (4:1) at 60 °C for 2 h, followed by precipitation with hexane, afforded

DOI: 10.1021/acs.inorgchem.5b01082
Inorg. Chem. 2015, 54, 6055–6061

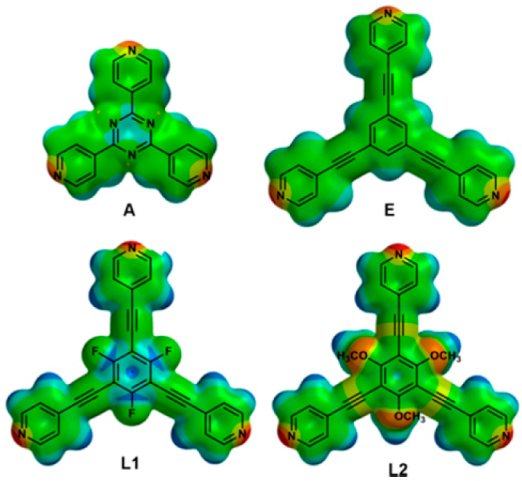

Figure 2. Electrostatic potential surfaces of **A**, **E**, **L1**, and **L2**. The structures are optimized at the B3LYP level of theory using the 6-31G* basis set in vacuum.[17] Red and blue represent negative and positive charge densities, respectively.

white solids **1a–b** and **2a–b** (Scheme 1). The ^{1}H NMR analysis shows one set of ligand proton signals indicating a highly symmetrical assembly (Figure 3a). The PyH_{α} signals of fluorine substituted cages are shifted downfield by ($\Delta\delta$) 0.36 (**1a**) and 0.30 ppm (**1b**), whereas the PyH_{β} signals move upfield by ($\Delta\delta$) −0.31 (**1a**) and −0.35 (**1b**) ppm as a result of the metal–ligand complexation. Only one band is observed in the ^{1}H DOSY NMR spectra for fluorine cages **1a** and **1b** with diffusion coefficients (D) of 2.35 × 10^{-10} m^2s^{-1} (**1a**, Figure 3b) and 2.29 × 10^{-10} m^2 s^{-1} (**1b**, Figure 3c), which correspond to spherical hydrodynamic diameters of 3.5 (**1a**) and 3.6 nm (**1b**). Similarly, for the methoxy substituted cages, **2a** and **2b**, complexation was confirmed by ^{1}H NMR (Figures S4, S16, and S21). Also, the hydrodynamic diameters obtained by ^{1}H DOSY NMR were similar in size, viz. 3.3 nm (**2a**) and 3.6 nm (**2b**) with the corresponding fluorine-containing cages (Figures S20 and S25). The hydrodynamic diameters are fully consistent with crystal structures of **1a** and **2a** as well as with the diameters calculated from collision cross sections (CCS) obtained from the ion-mobility mass spectrometry (IM-MS) experiments (see below, Table 1). The ^{31}P NMR (Figures S9, S14, S19, and S24) and ^{19}F NMR spectra (Figures S8 and S13) also support the formation of a single, highly symmetrical product.

Crystallography. Despite the 20-year history of M_6L_4 cages, surprisingly few good quality crystal structures have been published. Several crystal structures of complexes with the triazine ligand **A** were reported by Fujita et al. in 2002.[20] The electron-deficient Pd_6L_4 (L = the triazine **A**) cage with the cavity volume of ca. 750 Å^3 exhibits rich host–guest chemistry due to the suitably sized cavity for complete encapsulation of one, two, or four electron-rich guest molecules, depending on the size of the guest, viz. one tetrabenzylsilane (molecular volume = MV = 458 Å^3) or tri-*tert*-butylbenzene (MV = 320 Å^3), two diphenylmethane (MV = 202 Å^3) or 1,2-bis(4-methoxyphenyl)-1,2-ethanedione (MV = 279 Å^3) or four *o*-carborane (MV = 172 Å^3) or 1-adamantanol molecules (MV = 172 Å^3). A smaller version of the M_6L_4 cage with the cavity volume of ca. 500 Å^3 using tricyanobenzene (Figure 1, ligand **F**) as the ligand has been reported by Lusby et al.[12d] Their cage encapsulates four triflate anions (MV = 86 Å^3) symmetrically arranged around the center of the cavity. The largest M_6L_4 cage with 1,3,5-tris(4-pyridylethynyl)benzene (Figure 1, ligand **E**) and 1,3,5-tris(4-pyridyl-*trans*-ethenyl)benzene (Figure 1, ligand **G**) as the ligands has been reported by Stang et al.[12c] Because of the very large size of the cavity, large apertures (windows), and moderate crystal quality, no solid state host–guest complexation was observed. The overall size of the cavities of M_6L_4 cages made by Stang et al. is comparable to the cages **1a** and **2a** reported in this work; only the windows are smaller in **1a** and **2a** (see below).

Since only weak diffraction was observed with crystals of **1a** and **2a** (Figure 4), obtained by slow diffusion of hexane (**1a**) or acetone (**2a**) into a $CHCl_3$:CH_3OH (4:1) solution, the data collections were done using synchrotron radiation (see Supporting Information). In spite of numerous attempts with several different crystallization conditions, the corresponding Pd_6L_4 cages **1b** and **2b** did not form single crystals, and only powdery precipitate was obtained.

The Pt_6L_4 complexes **1a** and **2a** are discrete self-assembled supramolecular cages with an octahedral overall structure. The four pseudotrigonal ligands (**L1** or **L2**) form a large octahedrally shaped cavity with a radius of 8 Å (measured from the center of the cavity to the centroids of the central benzene ring of the paneling ligand) and volume of ca. 2000 Å^3.

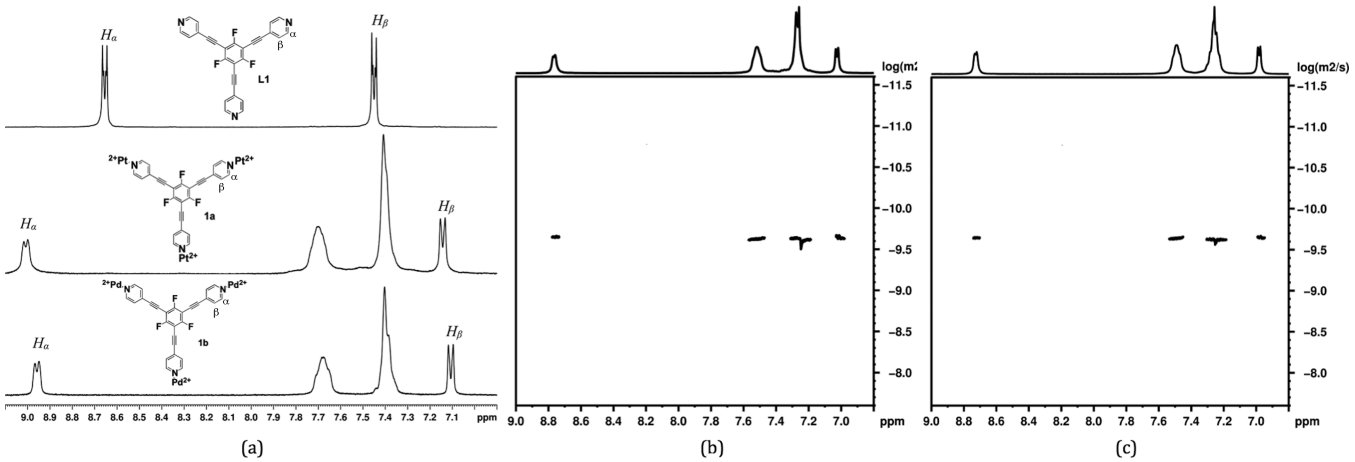

Figure 3. (a) Partial ^{1}H NMR (300 MHz, CD_2Cl_2, 303 K) spectra of ligand **L1**, cages **1a** and **1b** (top to bottom). Partial ^{1}H DOSY NMR (400 MHz, $CDCl_3$:CD_3OD 4:1, 298 K) spectra of cages (b) **1a** and (c) **1b**.

DOI: 10.1021/acs.inorgchem.5b01082
Inorg. Chem. 2015, 54, 6055–6061

Table 1. CCS_{exp} Values of $[M_6L_4(OTf)_8]^{4+}$ Ions and Comparison of Diameters Obtained by IM-MS, ^1H DOSY NMR and X-ray Diffraction

cage	m/z[a]	ion	CCS_{exp} (Å^2)[b]	IM-MS d (nm)[c]	DOSY d (nm)[d]	X-ray d (nm)[e]
1a	1645	$[Pt_6\mathbf{L1}_4(OTf)_8]^{4+}$	926 (mi)	3.4	3.5	3.7
			945 (ma)	3.5		
1b	1512	$[Pd_6\mathbf{L1}_4(OTf)_8]^{4+}$	962 (mi)	3.5	3.6	
			982 (ma)	3.5		
2a	1681	$[Pt_6\mathbf{L2}_4(OTf)_8]^{4+}$	965 (ma)	3.5	3.3	3.6
			988 (mi)	3.5		
2b	1548	$[Pd_6\mathbf{L2}_4(OTf)_8]^{4+}$	989 (ma)	3.6	3.6	
			974 (mi)	3.5		

[a]Most abundant m/z. [b]ma = major conformer, mi = minor conformer in ion mobilogram. [c]Calculated on the basis of CCS by assuming a spherical shape of the metal cage. [d]Calculated using Stokes−Einstein equation. [e]The average of the distance of the opposite H atoms +1.2 Å.

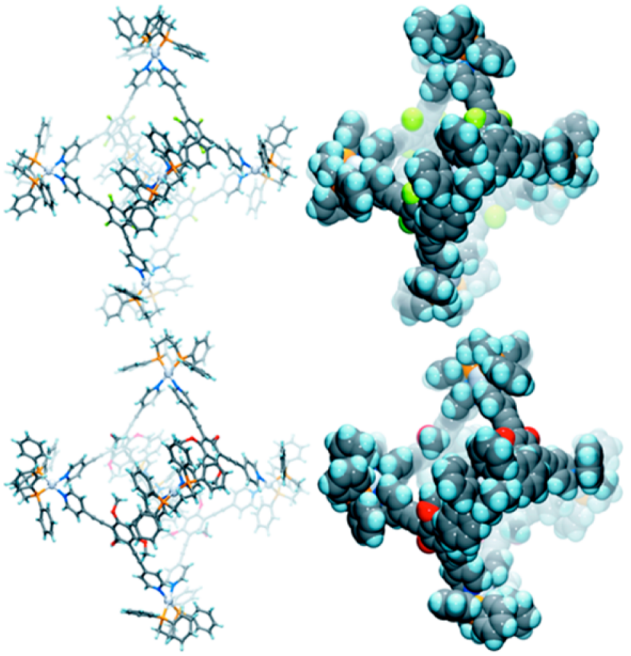

Figure 4. Crystal structures of **1a** (top) and **2a** (below), ball-and-stick (left), and space-filling models (right).

The cages have four large similar trigonal apertures, "windows", with a diameter of ca. 11 Å (Figure S26), the size of the windows being slightly smaller in **2a** due to the methoxy substituents. Nine out of the 12 methoxy substituents in the central benzene rings point toward the interior of the cavity **2a**, two pointing outside and one parallel with the benzene ring.

The X-ray structure of the uncomplexed ligand **L1** (Figures S27−S28) reveals the ligand itself to have a pseudotrigonal structure, showing marked deviations from the optimal 120° angles. The angles between the central benzene ring and the pyridine rings (Bz-Py, Figure S29) vary from 105.1 to 131.1°. This is also reflected in the N···N distances which vary from 13.09 to 15.00 Å (Figure S30), whereas the calculated structure of **L1** (obtained using *SPARTAN*[17]) shows N···N distances of 14.30 Å with a perfect trigonal symmetry. In addition to the deviation from the trigonal angles, also small deviations from planarity are observed (Figure S31), with the twist angle between the pyridine ring and the central 2,4,6-trifluorobenzene ring varying from −0.6 to +14.75°, the planarity being enhanced by quite strong $\pi-\pi$ interactions observed in the crystal lattice of **L1**. Upon complexation with the Pt- or Pd-corner complexes the ligands **L1** and **L2** adopt a more trigonal structure resulting in a coordination cage, which only slightly deviates from a regular octahedron. The four ligands and the four windows have all nearly the same dimensions, viz. ca. 14.5 Å, with N···N distances within the ligand varying from 13.73 to 14.64 Å for **1a** and 13.73 to 14.77 Å for **2a**. The trigonal angles in the cages **1a** and **2a** approach the ideal values, now being 111.7−127.6° for **1a** and 115.1−128.2° for **2a**. The lack of short contacts in the crystal structures of cages **1a** and **2a** allows a small twisting of the pyridine rings with respect to the central benzene ring, the twist angles varying from −12.3° to 5.13° for **1a** and −13.5° to 11.00° for **2a**.

Mass Spectrometry. The electrospray ionization mass spectra (ESI-MS) measured from 50 μM solutions of **1a**, **1b**, **2a**, and **2b** in CH_2Cl_2 show discrete peaks corresponding to ions $[M_6L_4(OTf)_{12-n}]^{n+}$ (n = 3−5) (Figures 5a, S32, S33).

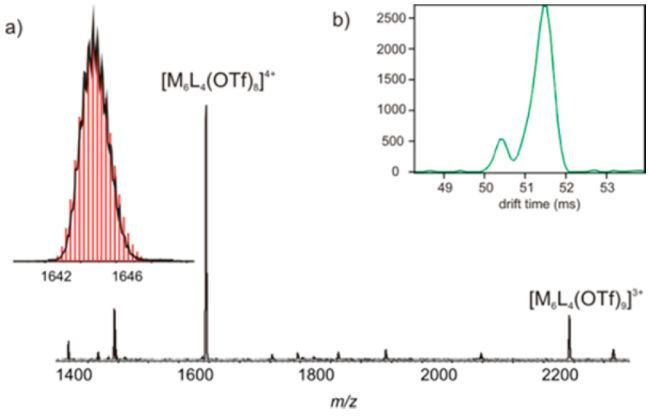

Figure 5. (a) ESI-TOF MS spectrum of **1a** (50 μM in CH_2Cl_2). Inset shows the fit of theoretical isotopic distribution (red solid line) (b) ion mobilogram (green line) for ion m/z 1644 corresponding to $[(dppp)Pt_6(\mathbf{L1})_4(OTf)_8]^{4+}$.

Intact M_6L_4 cages were observed as major products in each spectrum, although minor peaks for M_5L_4, M_4L_4, and M_4L_3 were evident, especially in samples of more labile Pd-cages. These smaller ions do not necessarily originate from fragmentation, but they may result from the instability of cages in μM-regime concentration used in the ESI-MS experiments, which is a common outcome with coordination complexes.[21]

The drift tube ion-mobility mass spectrometry (IM-MS) experiments confirmed $[M_6L_4(OTf)_{12-n}]^{n+}$ ions to have CCS values consistent with the crystal structures and the hydrodynamic diameters obtained by ^1H DOSY NMR (Table 1). Assuming a spherical shape for M_6L_4 cages, the diameters

DOI: 10.1021/acs.inorgchem.5b01082
Inorg. Chem. 2015, 54, 6055−6061

obtained from the crystal structures, hydrodynamic diameters (DOSY NMR) and the CCS-derived diameters (IM-MS) were all within 0.1−0.3 nm of each other. The values obtained with different techniques and in different states of matter are similar, indicating that any of these methods will give reliable results when carefully executed.[22]

As the drift tube of the IM-MS instrument is operated at atmospheric pressure, it allows high resolution separations and therefore accurate determination of CCS values without the need for cumbersome calibration, which often severely complicates the analysis done by using more common traveling-wave ion mobility MS (TWIM-MS).[22b] Consequently, the drift tube IM-MS is an ideal method to study gas phase shape and CCS values of metal cages with high resolution. It should be emphasized that IM-MS has not yet been widely applied to study gas-phase conformations of metal−organic cages or metal−organic structures.[22,23] Therefore, the comparison of CCS values with the DOSY NMR and crystal structures underlines the potential of IM-MS and verifies its applicability to structural studies of metal−organic cages. Especially when characterization through traditional methods (X-ray and NMR spectroscopy) is challenging or impossible, the IM-MS appears to be a highly valuable alternative.

For each $[M_6L_4(OTf)_8]^{4+}$ ion, two conformers were observed in ion mobilograms, one major and one minor (Figure 5b, S39). In most cases, the major conformer constituted ca. 80% of ion population, and the difference in CCS values between the conformers was only ca. ± 20 Å^2 (ca. 4−5 Å in diameter). It is, therefore, reasonable to assume that the conformations arise from variation in locations of the two triflate anions which exceed the number of metal centers in $[M_6L_4(OTf)_8]^{4+}$. This is also supported by the mobilogram of $[M_5L_4(OTf)_6]^{4+}$ (Figure S39) which shows only a single conformer (only one triflate exceeding the number of metal corners).

The isolated $[M_6L_4(OTf)_8]^{4+}$ ions were further studied in the gas phase by collision induced dissociation (CID) experiments (Figure 6, S36). In the qualitative sense, all metal cages

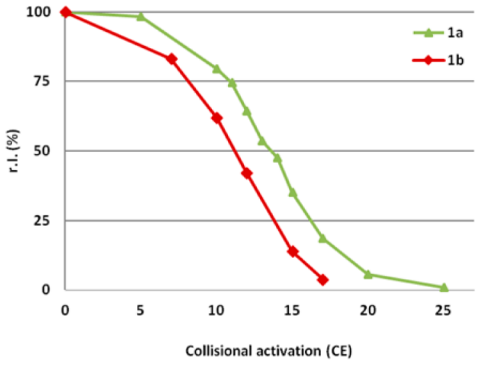

Figure 6. CID dissociation curves of isolated ions $[M_6L_4(OTf)_8]^{4+}$ for cages **1a** and **1b**.

dissociated similarly and produced structurally characteristic fragment ions through eliminations of $[M(OTf)]^+$, $[ML(OTf)]^+$, and $[M_2L(OTf)_2]^{2+}$. The elimination of two metal corners at most was in every case followed by elimination of a ligand, which is well in line with the cage-like structure. The experiments as a function of increased collisional activation revealed a clear stability difference between cages **1a** and **1b**, the former being more stable (Figure 6). Between cages **2a** and **2b**, such a stability difference was not observed (Figure S36). This behavior can be rationalized through stability differences between the metal corners. Because of the electron-withdrawing nature of ligand **L1**, the properties of metal−nitrogen bonds are more reflected in the overall gas phase stability of the cage. The differences between the two metal centers are also reflected in the experimental CCS values; the Pt-cages showing smaller CCS values (shorter coordinative bonds) compared to the corresponding Pd-cages. In addition, the difference between the CCS values in Pd- and Pt-cages with ligand **L1** is evidently larger compared to same difference between cages with **L2** (Table 1).

The mixed ligand experiment (both ligands present in equimolar ratio) further confirmed the ability of the both ligands to form a cage with Pt(II), with the formation of all three possible heterometallic cages $[M_6\mathbf{L1}_n\mathbf{L2}_{4-n}]$ (n = 0−4) observed experimentally (Figure S37). The formation of cages with ligand **L2** was only slightly favored over statistical distribution. A similar mixed-metal experiment (both metals present in equimolar ratio with one ligand) showed also close-to-statistical distribution of heterometallic cages (Figure S38), although the abundance of the cages was drastically lower compared to ones formed with only one metal. In the heterometallic experiment there was also increased abundance of the M_5L_4 fragments. This indicates a decreased stability of heterometallic cages, most probably due to slight distortion of cage. In addition, the observation of close-to-statistical distribution implies kinetic control in the formation of cages.

Photophysics. Distinct differences were observed in the absorption spectra of ligands **L1** and **L2** (Figure 7a). Electron-deficient **L1** showed two sharp absorption bands of similar

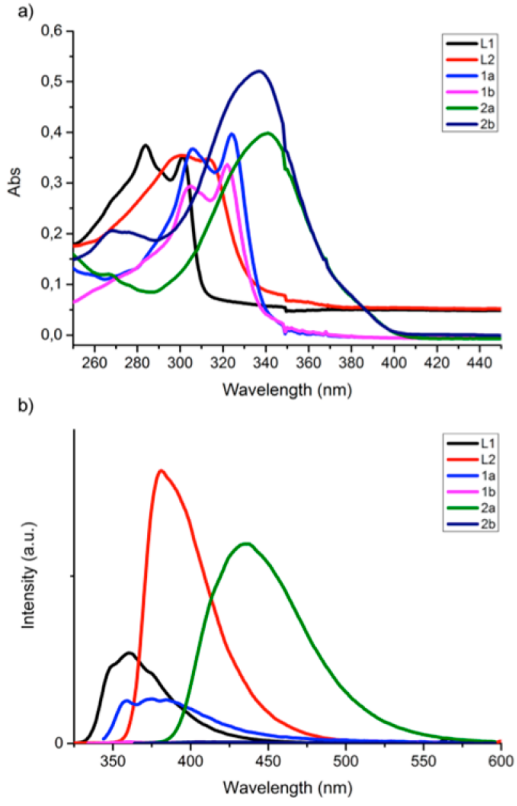

Figure 7. (a) Absorption and (b) emission spectra of ligands (4 μM) and cages (1 μM) in CH_2Cl_2.

DOI: 10.1021/acs.inorgchem.5b01082
Inorg. Chem. 2015, 54, 6055−6061

intensity at 284 and 301 nm (Table 2). A relatively broad shoulder was observed around 269 nm with a slightly lower

Table 2. Photophysical Properties of Ligands and Cages

	λ_{max} Abs (nm)	molar extinction coefficient (ε) (cm^{-1} mol^{-1})	λ_{max} Em (nm)	quantum yield Φ (%)
L1	269	67600	350	11.5
	284	93700	360	
	301	87900	375	
L2	303	88400	380	45.3
	313	86500		
1a	306	367000	358, 375, 385	8.0
	324	397000		
1b	305	294000	nop[a]	
	322	336000		
2a	341	398000	438	36.3
2b	337	521000	nop[a]	

[a]No observable peak.

intensity. The more electron-rich system **L2** showed broader, low-energy, almost equally intense absorption bands at 303 and 313 nm. A starker contrast was observed in the emission spectra of the two ligands (Figure 7b). The observed Stokes shifts were to a similar extent of 70−80 nm for both of the ligands. However, **L2** had a typical broad spectra centered around 380 nm, whereas **L1** showed a structured emission with three peaks at 350, 360, and 375 nm. This was distinctly different from the modestly broad, unstructured spectra observed for analogous compounds.[16] The quantum yield of **L2** was found to be significantly higher than **L1** (Table 2), which was in good agreement with reported values for similarly substituted 1,3,5-tris(ethynylphenyl)benzene analogues.[16]

The corresponding Pt- and Pd-cages (M_6L_4) for ligands **L1** and **L2** showed distinctly broader absorption spectra with characteristic red shifts to that of the free ligands (Figure 7a). Both Pt and Pd-cages of **L2**, **2a**, and **2b**, showed a broad absorption peak at 341 and 337 nm, respectively, with markedly higher intensity than the free ligands (Table 2). However, the corresponding cages of **L1**, **1a**, and **1b**, had similar absorption profiles characterized by two almost equally intense peaks. The **1a** showed two absorption bands at 306 and 324 nm, while the corresponding bands appeared at 305 and 322 nm for **1b**.

It can be argued that the absorbance spectra of the cages are ligand-centric and are weakly affected by coordinated metals. However, the emission spectra of the cages were critically influenced by the metal. While Pt-cages showed moderate to high emission intensity, especially in case of **2a**, Pd coordination drastically quenched any fluorescence from the ligands (Figure 7b). Cage **1a** showed a broad spectrum with vibrational structure with peaks at 358, 375, and 385 nm. The emission spectrum of **2a** was devoid of any vibrational structure and was centered around 438 nm.

CONCLUSIONS

The modular approach in the design of two new C_3-symmetric ligand for the construction of M_6L_4 coordination cages is presented. Either electron-withdrawing fluorine or electron-donating methoxy substituents modulate the electronic properties of the ligand, and thus electron-deficient (**1a** and **1b**) and electron-rich (**2a** and **2b**) M_6L_4 cages are obtained. Crystal structures of Pt-cages **1a** and **2a** expectedly showed them to be octahedral with a large open cavity punctured by four apertures. The host−guest chemistry studies of the cages will be presented in a future publication. In gas phase, collision cross section-based diameters for all cages were obtained by drift tube ion-mobility mass spectrometry (IM-MS). Moreover, using the collision-induced dissociation (CID) of the parent cage ions, the relative stabilities of the complexes in the gas phase could be established and correlated with the electronic properties of the ligands as well as the nature of the metal centers.

Detailed solution studies by NMR proved the highly symmetrical structure of the M_6L_4 cages and gave the hydrodynamic diameters in very good agreement with the values obtained in solid state and gas phase studies.

The photophysical properties of the ligands and the corresponding cages were shown to be critically dependent on the substituents on the core benzene ring. The ligands, especially electron-rich **L2** and the corresponding Pt-cage (**2a**), were shown to be strongly emissive and could be used in the future to develop capsules that act as fluorosensors upon guest encapsulation.

Our results highlight the importance of the combined structural studies of metallosupramolecular assemblies in the solid state, solution, and gas phase, particularly emphasizing the applicability and reliability of the ion-mobility mass spectrometry (IM-MS) in the structural studies of supramolecular coordination complexes.

ASSOCIATED CONTENT

Supporting Information

Experimental procedures, synthesis, and characterization data for ligands and M_6L_4 cages, and their MS, IM-MS, and X-ray diffraction data. The Supporting Information is available free of charge on the ACS Publications website at DOI: 10.1021/acs.inorgchem.5b01082.

AUTHOR INFORMATION

Corresponding Author

*E-mail: kari.t.rissanen@jyu.fi.

Funding

The Academy of Finland (K.R.: nos. 265328 and 263256; E.K: nos. 284562 and 278743). University of Jyväskylä (K.R.: Academy professorship support) Japanese Ministry of Education, Culture, Sports, Science, and Technology (MEXT) (SS.: nos. 25102007, 24685010 and. 2013G640).

Notes

The authors declare no competing financial interest.

ACKNOWLEDGMENTS

The authors kindly acknowledge the Academy of Finland (K.R.: nos. 265328 and 263256; E.K.: nos. 284562 and 278743), the University of Jyväskylä and the Japanese MEXT KAKENHI (S.S.: nos. 25102007 and 24685010). The synchrotron X-ray crystallography was performed at the BL1A beamline in KEK Photon Factory (S.S.: no. 2013G640).

REFERENCES

(1) (a) Cook, T. R.; Stang, P. J. *Chem. Rev.* **2015**, DOI: 10.1021/cr5005666. (b) Cook, T. R.; Zheng, Y.-R.; Stang, P. J. *Chem. Rev.* **2013**, *113*, 734. (c) Ronson, T. K.; Zarra, S.; Black, S. P.; Nitschke, J. R. *Chem. Commun.* **2013**, *49*, 2476. (d) Chakrabarty, R.; Mukherjee, P. S.; Stang, P. J. *Chem. Rev.* **2011**, *111*, 6810. (e) Ward, M. D. *Chem. Commun.* **2009**, *30*, 4487. (f) Saalfrank, R. W.; Maid, H.; Scheurer, A. *Angew. Chem., Int. Ed.* **2008**, *47*, 8794. (g) Seidel, S. R.; Stang, P. J. *Acc.*

DOI: 10.1021/acs.inorgchem.5b01082
Inorg. Chem. 2015, 54, 6055−6061

Chem. Res. **2002**, *35*, 972. (h) Caulder, D. L.; Brückner, C.; Powers, R. E.; König, S.; Parac, T. N.; Leary, J. A.; Raymond, K. N. *J. Am. Chem. Soc.* **2001**, *123*, 8923. (i) Leininger, S.; Olenyuk, B.; Stang, P. J. *Chem. Rev.* **2000**, *100*, 853. (j) Stang, P. J.; Olenyuk, B. *Acc. Chem. Res.* **1997**, *30*, 502.

(2) (a) Olenyuk, B.; Whiteford, J. A.; Fechtenkotter, A.; Stang, P. J. *Nature* **1999**, *398*, 796. (b) Ghosh, K.; Hu, J.; White, H. S.; Stang, P. J. *J. Am. Chem. Soc.* **2009**, *131*, 6695. (c) Tominaga, M.; Suzuki, K.; Kawano, M.; Kusukawa, T.; Ozeki, T.; Sakamoto, S.; Yamaguchi, K.; Fujita, M. *Angew. Chem., Int. Ed.* **2004**, *43*, 5621. (d) Sun, Q. F.; Iwasa, J.; Ogawa, D.; Ishido, Y.; Sato, S.; Ozeki, T.; Sei, Y.; Yamaguchi, K.; Fujita, M. *Science* **2010**, *328*, 1144. (e) Bunzen, J.; Iwasa, J.; Bonakdarzadeh, P.; Numata, E.; Rissanen, K.; Sato, S.; Fujita, M. *Angew. Chem., Int. Ed.* **2012**, *51*, 3161.

(3) (a) Saalfrank, R. W.; Stark, A.; Peters, K.; von Schnering, H. G. *Angew. Chem., Int. Ed. Engl.* **1988**, *27*, 851. (b) Beissel, T.; Powers, R. E.; Raymond, K. N. *Angew. Chem., Int. Ed. Engl.* **1996**, *35*, 1084. (c) Caulder, D. L.; Powers, R. E.; Parac, T. N.; Raymond, K. N. *Angew. Chem., Int. Ed.* **1998**, *37*, 1840. (d) Fleming, J. S.; Mann, K. L. V.; Carraz, C.; Psillakis, E.; Jeffery, J. C.; McCleverty, J. A.; Ward, M. D. *Angew. Chem., Int. Ed.* **1998**, *37*, 1279. (e) Johnson, D. W.; Raymond, K. N. *Inorg. Chem.* **2001**, *40*, 5157. (f) Paul, R. L.; Bell, Z. R.; Jeffery, J. C.; McCleverty, J. A.; Ward, M. D. *Proc. Natl. Acad. Sci. U. S. A.* **2002**, *99*, 4883. (g) Clegg, J. K.; Lindoy, L. F.; Moubaraki, B.; Murray, K. S.; McMurtrie, J. C. *Dalton Trans.* **2004**, *16*, 2417. (h) Mal, P.; Schultz, D.; Beyeh, K.; Rissanen, K.; Nitschke, J. R. *Angew. Chem., Int. Ed.* **2008**, *47*, 8297. (i) Biros, S. M.; Yeh, R. M.; Raymond, K. N. *Angew. Chem., Int. Ed.* **2008**, *47*, 6062. (j) Saalfrank, R. W.; Maid, H.; Scheurer, A.; Heinemann, F. W.; Puchta, R.; Bauer, W.; Stern, D.; Stalke, D. *Angew. Chem., Int. Ed.* **2008**, *47*, 8941. (k) Mal, P.; Breiner, B.; Rissanen, K.; Nitschke, J. R. *Science* **2009**, *324*, 1697. (l) Liu, T.; Liu, Y.; Xuan, W.; Cui, Y. *Angew. Chem., Int. Ed.* **2010**, *49*, 4121. (m) Clegg, J. K.; Li, F.; Jolliffe, K. A.; Meehan, G. V.; Lindoy, L. F. *Chem. Commun.* **2011**, *47*, 6042. (n) Mahata, K.; Frischmann, P. D.; Würthner, F. *J. Am. Chem. Soc.* **2013**, *135*, 15656. (o) Ronson, T. K.; Giri, C.; Beyeh, N. K.; Minkkinen, A.; Topić, F.; Holstein, J. J.; Rissanen, K.; Nitschke, J. R. *Chem.—Eur. J.* **2013**, *19*, 3374. (p) Giri, C.; Topić, F.; Mal, P.; Rissanen, K. *Dalton Trans.* **2014**, *43*, 17889. (q) Frischmann, P. D.; Kunz, V.; Stepanenko, V.; Würthner, F. *Chem.—Eur. J.* **2015**, *21*, 2766. (r) Roukala, J.; Zhu, J.; Giri, C.; Rissanen, K.; Lantto, P.; Telkki, V.-V. *J. Am. Chem. Soc.* **2015**, *137*, 2464. (s) Giri, C.; Sahoo, P. K.; Puttreddy, R.; Rissanen, K.; Mal, P. *Chem.—Eur. J.* **2015**, *21*, 6390.

(4) (a) Amoroso, A. J.; Jeffery, J. C.; Jones, P. L.; McCleverty, J. A.; Thornton, P.; Ward, M. D. *Angew. Chem., Int. Ed. Engl.* **1995**, *34*, 1443. (b) Brückner, C.; Powers, R. E.; Raymond, K. N. *Angew. Chem., Int. Ed.* **1998**, *37*, 1837. (c) Saalfrank, R. W.; Glaser, H.; Demleitner, B.; Hampel, F.; Chowdhry, M. M.; Schünemann, V.; Trautwein, A. X.; Vaughan, G. M.; Yeh, R.; Davis, A. V.; Raymond, K. N. *Chem.—Eur. J.* **2002**, *8*, 493. (d) Albrecht, M.; Janser, I.; Meyer, S.; Weis, P.; Frohlich, R. *Chem. Commun.* **2003**, 2854. (e) Albrecht, M.; Janser, I.; Frohlich, R. *Chem. Commun.* **2005**, 157. (f) Yeh, R. M.; Xu, J.; Seeber, G.; Raymond, K. N. *Inorg. Chem.* **2005**, *44*, 6228. (g) Albrecht, M.; Janser, I.; Burk, S.; Weis, P. *Dalton Trans.* **2006**, *23*, 2875. (h) Granzhan, A.; Schouwey, C.; Riis-Johannessen, T.; Scopelliti, R.; Severin, K. *J. Am. Chem. Soc.* **2011**, *133*, 7106. (i) Bilbeisi, R. A.; Clegg, J. K.; Elgrishi, N.; Hatten, X. d.; Devillard, M.; Breiner, B.; Mal, P.; Nitschke, J. R. *J. Am. Chem. Soc.* **2012**, *134*, 5110. (j) Albrecht, M.; Shang, Y.; Hasui, K.; Gossen, V.; Raabe, G.; Tahara, K.; Tobe, Y. *Dalton Trans.* **2012**, *41*, 9316. (k) Albrecht, M.; Shang, Y.; Rhyssen, T.; Stubenrauch, J.; Winkler, H. D. F.; Schalley, C. A. *Chem.—Eur. J.* **2012**, *2012*, 2422.

(5) (a) Roche, S.; Haslam, C.; Heath, S. L.; Thomas, J. A. *Chem. Commun.* **1998**, 1681. (b) Suzuki, K.; Tominaga, M.; Kawano, M.; Fujita, M. *Chem. Commun.* **2009**, 1638.

(6) (a) Bell, Z. R.; Harding, L. P.; Ward, M. D. *Chem. Commun.* **2003**, 2432. (b) Browne, C.; Brenet, S.; Clegg, J. K.; Nitschke, J. R. *Angew. Chem., Int. Ed.* **2013**, *52*, 1944. (c) Najar, A. M.; Tidmarsh, I. S.; Adams, H.; Ward, M. D. *Inorg. Chem.* **2009**, *48*, 11871.

(7) (a) Natarajan, R.; Savitha, G.; Moorthy, J. N. *Cryst. Growth Des.* **2005**, *5*, 69. (b) Johannessen, S. C.; Brisbois, R. G.; Fischer, J. P.; Grieco, P. A.; Counterman, A. E.; Clemmer, D. E. *J. Am. Chem. Soc.* **2001**, *123*, 3818.

(8) Meng, W.; Breiner, B.; Rissanen, K.; Thoburn, J. D.; Clegg, J. K.; Nitschke, J. R. *Angew. Chem., Int. Ed.* **2011**, *50*, 3479.

(9) Fujita, M.; Oguro, D. *Nature* **1995**, *378*, 469.

(10) Stang, P. J.; Olenyuk, B.; Muddiman, D. C.; Smith, R. D. *Organometallics* **1997**, *16*, 3094.

(11) Stang, P. J.; Huang, Y.-H.; Arif, A. M. *Organometallics* **1992**, *11*, 231.

(12) (a) Yamashita, K.; Sato, K.; Kawano, M.; Fujita, M. *New J. Chem.* **2009**, *33*, 264. (b) Leininger, S.; Fan, J.; Schmitz, M.; Stang, P. J. *Proc. Natl. Acad. Sci. U. S. A.* **2000**, *97*, 1380. (c) Schweiger, M.; Yamamoto, T.; Stang, P. J.; Bläser, D.; Boese, R. *J. Org. Chem.* **2005**, *70*, 4861. (d) Chepelin, O.; Ujma, J.; Wu, X.; Slawin, A. M. Z.; Pitak, M. B.; Coles, S. J.; Michel, J.; Jones, A. C.; Barran, P. E.; Lusby, P. J. *J. Am. Chem. Soc.* **2012**, *134*, 19334.

(13) (a) Hartshorn, C. M.; Steel, P. J. *Chem. Commun.* **1997**, 541. (b) Fujita, M.; Yu, S.; Kusukawa, T.; Funaki, H.; Ogura, K.; Yamaguchi, K. *Angew. Chem., Int. Ed.* **1998**, *37*, 2082. (c) Schmittel, M.; He, B.; Fan, J.; Bats, J. W.; Engeser, M.; Schlosser, M.; Deiseroth, H. *Inorg. Chem.* **2009**, *48*, 8192. (d) Peuronen, A.; Forsblom, S.; Lahtinen, M. *Chem. Commun.* **2014**, *50*, 5469.

(14) (a) Kusukawa, T.; Fujita, M. *J. Am. Chem. Soc.* **2002**, *124*, 13576. (b) Fang, Y.; Murase, T.; Sato, S.; Fujita, M. *J. Am. Chem. Soc.* **2013**, *135*, 613. (c) Fang, Y.; Murase, T.; Fujita, M. *Chem.—Asian J.* **2014**, *9*, 1321.

(15) Yamashita, K.; Kawano, M.; Fujita, M. *Chem. Commun.* **2007**, *40*, 4102.

(16) Hennrich, G.; Asselberghs, I.; Clays, K.; Persoons, A. *J. Org. Chem.* **2004**, *69*, 5077.

(17) *SPARTAN '14*; Wavefunction Inc.: Irvine, CA, 2014.

(18) (a) Ohmori, O.; Kawano, M.; Fujita, M. *J. Am. Chem. Soc.* **2004**, *126*, 16292. (b) Ikemoto, K.; Inokuma, Y.; Fujita, M. *J. Am. Chem. Soc.* **2011**, *133*, 16806.

(19) (a) Kumazawa, K.; Biradha, K.; Kusukawa, T.; Okano, T.; Fujita, M. *Angew. Chem., Int. Ed.* **2003**, *42*, 3909. (b) Yoshizawa, M.; Nakagawa, J.; Kumazawa, K.; Nagao, M.; Kawano, M.; Ozeki, T.; Fujita, M. *Angew. Chem., Int. Ed.* **2005**, *44*, 1810. (c) Murase, T.; Otsuka, K.; Fujita, M. *J. Am. Chem. Soc.* **2010**, *132*, 7864.

(20) Kusukawa, T.; Fujita, M. *J. Am. Chem. Soc.* **2002**, *124*, 13576.

(21) Qi, Z.; Heinrich, T.; Moorthy, S.; Schalley, C. A. *Chem. Soc. Rev.* **2015**, *44*, 515.

(22) (a) Chan, Y.; Li, X.; Yu, J.; Carri, G. A.; Moorefield, C. N.; Newkome, G. R.; Wesdemiotis, C. *J. Am. Chem. Soc.* **2011**, *133*, 11967. (b) Wang, M.; Wang, C.; Hao, X.; Li, X.; Vaughn, T. J.; Zhang, Y.; Yu, Y.; Li, Z.; Song, M.; Yang, H.; Li, X. *J. Am. Chem. Soc.* **2014**, *136*, 10499. (c) Brocker, E. R.; Anderson, S. E.; Northrop, B. H.; Stang, P. J.; Bowers, M. T. *J. Am. Chem. Soc.* **2010**, *132*, 13486.

(23) (a) Tsybizova, A.; Rulíšek, L.; Schröder, D.; Rokob, T. A. *J. Phys. Chem. A* **2013**, *117*, 1171. (b) Ujma, J.; De Cecco, M.; Chepelin, O.; Levene, H.; Moffat, C.; Pike, S. J.; Lusby, P. J.; Barran, P. E. *Chem. Commun.* **2012**, *48*, 4423.

DOI: 10.1021/acs.inorgchem.5b01082
Inorg. Chem. 2015, 54, 6055−6061